J Therm Spray Tech (2020) 29:908–920
https://doi.org/10.1007/s11666-020-01045-2

PEER REVIEWED

Online Diagnostic System to Monitor Temperature of In-Flight Particles in Suspension Plasma Spray

A. Akbarnozari[1] · F. Ben-Ettouil[1] · S. Amiri[1] · O. Bamber[2] · J.-D. Grenon[2] · M. Choquet[2] · L. Pouliot[2] · C. Moreau[1]

Submitted: 25 October 2019 / in revised form: 29 April 2020 / Published online: 17 May 2020

Abstract Suspension plasma spray (SPS) is going through a transition phase from research and development to daily use on production lines. Improving repeatability and reproducibility of coating elements and parameters makes SPS a replacement of former well-developed processes. This transition can be achieved by using in-flight particles diagnostic systems to monitor and control key parameters that influence the coating microstructure. Temperature and velocity of the in-flight particles are among the most critical parameters that should be monitored. However, accurately characterizing the in-flight particles in SPS is particularly challenging due to the small particle size of coating materials, harsh spray conditions, considerably shorter spray distances compared to APS, possible interference from the solvent, and limitations of previous measurement systems. In this study, different strategies were investigated to improve the accuracy of temperature measurements of in-flight particles in SPS. For this purpose, two light collection configurations (double-point and single-point measurement) were investigated along with the influence of plasma radiation. The results were evaluated by collecting and studying splats. The size and shape of splats were correlated with the temperature of in-flight particles in order to confirm the accuracy of the sensor's temperature measurements. In addition, the sensitivity of temperature measurements to the optical filter used for two-color pyrometry, reflection of plasma radiation from surrounding objects, and direct radiation from plasma were investigated. The results showed that the single-point measurement configuration was well adapted for SPS.

Keywords diagnostic system · online measurement · in-flight particle temperature · suspension plasma spray · thermal emission · two-color pyrometer

Introduction

Suspension plasma spray (SPS) produces coatings with unique microstructures achieved by injecting submicron ceramic particles through a liquid carrier in a high-temperature plasma jet. The SPS coatings display superior chemical, mechanical, and thermal properties which opens opportunities for numerous applications (Ref 1). Temperature and velocity of in-flight particles in SPS are among the main parameters controlling the coating microstructure and, consequently, its overall properties of the surface. The condition of the in-flight particles before impingement on the substrate has a direct impact on the coating characteristics (Ref 2). Therefore, to control hardness, thermal conductivity, and other properties of the final coating, temperature and velocity of in-flight particles are key parameters that should be monitored and controlled (Ref 3). Regarding the importance of online monitoring systems, on the one hand, these tools have become an important component for developing, understanding, and optimizing new processes in research, and on the other

This article is an invited paper selected from presentations at the 2019 International Thermal Spray Conference, held May 26-29, 2019 in Yokohama, Japan and has been expanded from the original presentation.

✉ A. Akbarnozari
christian.moreau@concordia.ca; anozari007@gmail.com

[1] Department of Mechanical, Industrial, and Aerospace Engineering, Concordia University, Montreal, QC H3G 1M8, Canada

[2] Tecnar Automation Ltée, Saint-Bruno-de-Montarville, QC J3V 6B5, Canada

hand, they have been crucial for the advancement of automation in industrial production lines. In short, monitoring tools facilitate understanding the process–property correlation (Ref 4). Development of diagnostic tools and measurement setups for different thermal spray processes has been investigated by several authors including Solonenko (Ref 5), Boulos (Ref 6, 7), Fincke (Ref 8, 9), and Vardelle (Ref 10). Fauchais et al. (Ref 11) and Mauer et al. (Ref 12, 13) reviewed research and development of diagnostic systems of in-flight particles, and they tabulated the methods in terms of measurement of temperature, velocity, size, number density, and shape. Moreau et al. (Ref 14-18) developed integrated velocity and temperature measurement systems that led to the commercialization the DVP-2000 and AccuraSpray sensors (Tecnar, Canada). The DPV-2000 was the first commercial diagnostic system specifically designed for the characterization of thermal spray processes. It is based on a single-counting measurement with a two-slit mask at the tip of an optical fiber in the sensor head to characterize particles between 10 and 100 μm. It has a two-color pyrometer to measure temperature. The AccuraSpray (Ref 18) was designed as an industrial diagnostic tool to monitor spray conditions in atmospheric plasma spray (APS) and high velocity processes (HVOF) by measuring temperature and velocity of the in-flight particles as well as spray plume geometry. However, each process required an adapted sensor head because of different filtering requirements. The AccuraSpray helped in research to investigate and optimize spray distance for SPS process (Ref 19). Mauer et al. (Ref 20) compared AccuraSpray with the DPV-2000 (Tecnar, Canada) for APS powders, and they found good agreement between the measured temperatures of in-flight particles by both systems. An imaging diagnostic system was developed based on works of Vattulainen et al. (Ref 21) and commercialized as SprayWatch (Oseir Ltd., Tampere, Finland). This system measures the particle temperature from long-exposure-time images for two-color pyrometry and the particle velocity by the length of the particle. ThermaViz (Ref 22, 23) (Stratonics Inc., CA, USA) is a two-wavelength imaging pyrometer to measure temperature. Based on the two-color pyrometry, the In-flight Particle Pyrometer (IPP) was developed based on the work of Swank et al. at Idaho National Engineering Laboratory. Wroblewski et al. (Ref 24) discussed correlating temperature of particles to the molten volume flux across the plume. All of these diagnostic systems are designed for particle diagnosis in thermal spray processes in general but not for SPS that relies on much smaller in-flight particles (0.5-5 μm). Furthermore, McDonald et al. (Ref 25) carried out splat studies and temperature measurement for the APS process. As an offline characterization method, Delbos et al. (Ref 26) sampled in-flight particles on a glass lamella at the tip of a moving pendulum and they measured the diameter of collected splats by atomic force microscopy (AFM). Zeng et al. (Ref 27) collected in-flight particles in liquid nitrogen for further analysis during the APS process. Tarasi et al. (Ref 28) took samples of in-flight particles of alumina–zirconia collected in water and determined the average size in scanning electron microscope (SEM) micrographs. They tried to relate the online measured temperature of in-flight particles to characteristics of the collected splats to confirm the validity of online measurements. To monitor the in-flight particles, there are some challenges that are unique to the SPS process. Small particles, rapid temperature change of the particles along the spray axis, thermal and nonthermal radiation from plasma (Ref 29) are some challenges of in-flight particles measurement in the SPS process. The AccuraSpray G3C (and earlier versions) is an ensemble particle diagnostic system relying on a double-point measurement configuration that was designed for conventional thermal spray processes and not for SPS process. The double-point measurement configuration consists in collecting the thermal radiation emitted by the in-flight particles at two different wavelengths at two locations spaced by a few millimeters along the particle jet. When it is applied to SPS, the sensor could lack accuracy especially for temperature measurement due to the considerable temperature gradient along the spray axis. Then, temperature of in-flight particles at these two points in space is different which may lead to loss in accuracy of the temperature measurement. AccuraSpray was used to study temperature and velocity of in-flight particles in SPS (Ref 19) in works of Tarasi et al. (Ref 28) and Vaβen et al. (Ref 30). However, the possibilities and limitations of these measurements need to be better studied in SPS conditions.

The main objective of this paper is to assess the reliability and accuracy of in-flight particle temperature measurement in SPS. To so do, comparison between double-point and single-point measurement configurations was carried out. Furthermore, effects of optical filtering, surrounding radiation reflection, and plasma radiation (direct and reflected) on raw signals and temperature measurement in the SPS process were investigated. Finally, the overall performance of the new AccuraSpray 4.0 based on the single-point measurement configuration in SPS processes was evaluated.

Theory and Background

Temperature Measurement

The temperature measurement using the AccuraSpray sensor is carried out by detecting the electromagnetic

radiation emitted from in-flight particles. The sensor provides an ensemble average data from particles that pass through its measurement volume which is roughly 200 mm3. The signal collected at each wavelength is the result of the integration of radiation from all the particles in the measurement volume. Since the signal does not belong to any single particle, the measurement represents the temperature of the ensemble of particles. The minimum measurable temperature for this apparatus is around 900 °C. It has a camera and an alignment beam to place the measurement volume at a target point. It measures the temperature by using a two-color pyrometer based on the Planck's law (Ref 31, 32). Briefly, the thermal radiation from a body is a function of wavelength, emissivity, and temperature as given in Eq. 1.

$$I_{\mathrm{em}}(\lambda, T) = \varepsilon \frac{C_1}{\lambda^5} \frac{1}{\left\{\exp \frac{C_2}{\lambda T} - 1\right\}} \mathrm{d}\lambda \qquad \text{(Eq 1)}$$

where I_{em} is the intensity emitted by a black body in W/Sr in an interval of wavelength d centered at a wavelength in meter, T is the particle's surface temperature in Kelvin, $C_1 = 9.352 \times 10^{-17}$ W m^2, $C_2 = 1.439 \times 10^{-2}$ m K, and ε is the emissivity. *A* two-color pyrometer measures the intensity of radiation I_{λ_1} and I_{λ_2} at two wavelengths λ_1 and λ_2. For this purpose, a bandpass filter is placed in front of each of two detectors to block other wavelengths. Generally, the radiant source is assumed to behave as a gray body. The temperature is calculated from Eq. 2.

$$T = \frac{C_2(\lambda_1 - \lambda_2)}{\lambda_1 \lambda_2} \cdot \left[\ln \frac{I_{\lambda_1}}{I_{\lambda_2}} + 5 \ln \frac{\lambda_1}{\lambda_2}\right]^{-1} \qquad \text{(Eq 2)}$$

Generally, temperature and velocity of in-flight particles together provide key characteristics of a spray condition. In the AccuraSpray system, the particle velocity is measured by a time-of-flight technique (Ref 15). Each particle in the measurement volume radiates a signal that passes through two adjacent measurement points located along to the direction of motion of the particle in the spray plume. Knowing the distance between the measurement points, the particle speed is calculated from the delay between detection of the arrival of the particles in each detector.

There is an uncertainty in the measurement of temperature by a two-color pyrometer. A fundamental assumption for temperature measurement is that in-flight particles are gray body. According to definition, emissivity of surface is independent of wavelengths for the gray body. However, emissivity at two wavelengths is not necessarily equal for real materials. Mauer et al. (Ref 33) studied temperature errors by deviations from the gray body assumption as a function of temperature as shown in Fig. 1. For example, 7.5% difference between emissivity at two wavelengths ($\varepsilon_{\lambda 1}/\varepsilon_{\lambda 2} = 0.925$) results around 200 °C error for a

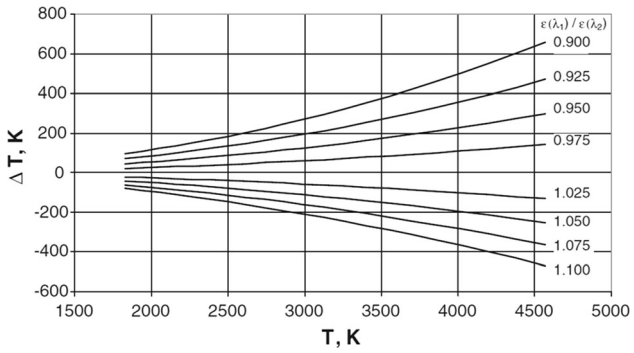

Fig. 1 Temperature measurement error as a function of emissivity ratios and absolute temperature

measurement at 3000 °C. Touloukian and DeWitt (Ref 34) studied the thermal properties for a wide range of materials. Manara et al. (Ref 35) reported emittance of YSZ as a function of wavelengths which is a common material in SPS. Therefore, deviation from gray body assumption can be further studied by considering emissivity ratio at two wavelengths ($\varepsilon_{\lambda 1}/\varepsilon_{\lambda 2}$).

Gray body assumption causes an uncertainty in temperature measurement of in-flight particles by the two-color pyrometer. The uncertainty of temperature measurement (ΔT) (Ref 36) arising from the unequal emissivity of ε_1 and ε_2 at two wavelengths of λ_1 and λ_2 is shown in Eq. 3.

$$c_2 \frac{\Delta T}{T^2} = \left(\frac{1}{\lambda_2} - \frac{1}{\lambda_1}\right)^{-1} \ln \frac{\varepsilon_2}{\varepsilon_1} \qquad \text{(Eq 3)}$$

where c and T are a constant and temperature, respectively. The uncertainty is minimum when the two wavelengths are close, and it increases as the separation between the two wavelengths increases. As determined by Planck's law, the sensitivity of a temperature measurement is a function of the radiation intensity ratio determined at two wavelengths ($I_{\lambda_2}/I_{\lambda_1}$). If the selected wavelengths are close to each other, the slope of the intensity ratio $I_{\lambda_2}/I_{\lambda_1}$ as a function of temperature is small, resulting in a low sensitivity of the two-color pyrometer measurements. As the distance between the two wavelengths increases, the slope of the intensity ratio as a function of temperature increases. If the slope is increased, small changes in temperature cause larger changes in the intensity ratio, which means a higher sensitivity of the device. However, minimizing the uncertainty by choosing closer wavelengths in the spectrum costs a loss in sensitivity of two-color pyrometer. Therefore, separated wavelengths are selected to have an effective sensitivity to measure temperature with an uncertainty estimated at ± 10 °C. The gray body assumption causes some uncertainty in measurement of the absolute temperature. However, relative temperature (temperature variations) can be determined reliably. In fact, the two-color pyrometer, which operates based on the gray body

assumption, effectively shows the trend of temperature and it responds appropriately to changes of measurement conditions such as a higher or a lower power and a shorter or a longer standoff distance. Therefore, the pyrometer based on the gray body assumption still provides a reliable relative temperature of in-flight particles.

Single-Point Measurement Versus Double-Point Measurement

Figure 2 shows a schematic diagram of a two-color pyrometer used in a double-point measurement configuration as implemented in the AccuraSpray G3C (and earlier versions) versus a single-point measurement configuration studied in this work and implemented in the new AccuraSpray 4.0. Contrary to the double-point measurement system, where I_{λ_1} and I_{λ_2} are measured at two distinct points along the spray axis (almost 3 mm apart from each other), in the single-point measurement system, the signal is captured from one point in the measurement volume and the collected radiation is split into two parts using a dichroic mirror. The signals are then passed through the bandpass filters to allow two distinct wavelengths to reach each detector. Aziz et al. (Ref 29) investigated the effect of plasma radiation on the accuracy of temperature measurements. Based on their finding, the bandpass filters were readjusted and optimized for more effective elimination of the plasma radiation. It is worth mentioning that double-point measurement system has some practical advantages in terms of robustness of measurement, relative simplicity of the configuration, and cost efficiency. In fact, the double-point measurement is a robust system that provides reliable result for APS and HVOF processes. Furthermore, it does not require a dichroic mirror in the configuration which makes it simpler, while the results are still reliable. Finally, from a commercial aspect, a double-point measurement system is less expensive to manufacture which was more favorable for customers and the developer.

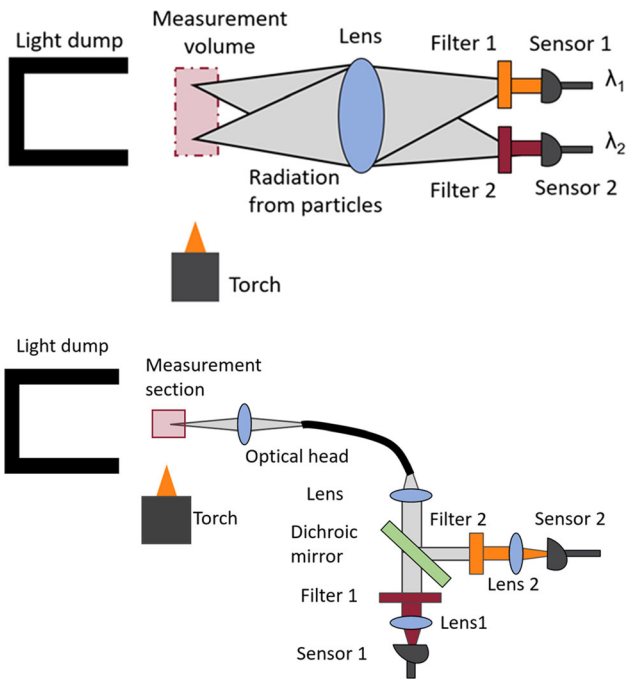

Fig. 2 Schematic diagram of the pyrometer for characterization of the particles configured with (top) double-point measurement of AccuraSpray G3C, (bottom) single-point measurement of the prototype and AccuraSpray 4.0

Velocity Measurement

For more extensive characterization of in-flight particles, temperature and velocity of particles are studied together. Velocity measurement was not the focus of this part, and the principle is explained in general terms. Velocity of in-flight particles is calculated by using a time-of-flight approach. Each particle in the measurement volume radiates a signal that passes through two adjacent measurement slits located parallel to the general motion of the particles in the spray plume. Knowing the distance between the measurement points and magnification of optics, the particle speed is calculated from the time difference between the radiation peaks measured in each detector.

Experimental Methodology

The three distinct diagnostic apparatuses used in our experiments were the double-point measurement AccuraSpray G3C, a new prototype of single-point measurement, and AccuraSpray 4.0 developed based on the prototype with a readjustment of transmission window for filtering (both center wavelength (CWL) and full width at half maximum (FWHM)).This paper reports two main sets of experiments. In the first part, temperature of the in-flight particles sprayed during the SPS process was evaluated by both the double-point measurement system and single-point measurement prototype. This prototype was used to assess the gain in accuracy of the single-point measurement approach over the two-point measurement. In fact, it served as a proof of concept in the development of the new AccuraSpray 4.0. In the second part, the SPS process was characterized by the single-point measurement system (AccuraSpray 4.0) equipped with an optimized filtering. Furthermore, the sensitivity of measurements to changes in spray and testing conditions was analyzed.

Comparison of AccuraSpray G3C and the Prototype in SPS

The AccuraSpray G3C based on the double-point measurement configuration and the single-point prototype was compared to measure temperature of in-flight particles related to changes of plasma power and standoff distance. The powder used for the experiment was 8 mol.% YSZ (ZiBo.V.Gree. Trading, China) with an average particle size 0.4 μm. A suspension of 1 wt.% polyvinylpyrrolidone (Sigma-Aldrich, USA) as a surfactant and 20 wt.% powder in ethanol was radially injected into the plasma jet originated from a 6 mm nozzle of a 3 MB torch (Oerlikon Metco, Switzerland). The suspension was feed at a constant flow rate of 25 mL/min, and the experiments were repeated for three different plasma powers which was adjusted by controlling the gas composition, gas flow rate, and electrical current of plasma. Table 1 shows the variables and spray conditions for each test.

Measurement by the Prototype and Splats Sampling

Validity of the temperature measurements was indirectly investigated by studying the splats obtained in the different spray conditions. To generate the splats samples, the suspension was prepared as described above, but the powder concentration was set to 10 wt.%. Lower suspension concentration was used to reduce the density of splats collected on glass substrates. For the purpose of validation, the temperature was measured using the prototype at five different spray distances and splat samples were collected on a glass substrate at the same distances. The spray parameters of these experiments were those identified as Test #3 in Table 1. The collected splats were studied by using a scanning electron microscope (SEM) S3400 (Hitachi, Japan) at accelerating voltage of 5 kV. Then, correlation between the measured temperatures of in-flight particles and micrographic information from the collected splat samples were studied.

Table 1 Plasma conditions for spraying the YSZ suspension with the 3 MB torch

Test #	Gas flow rate, L/min			Current, A	Power, kW
	Ar	He	H2		
1	45	0	5	600	34
2	25	25	0	700	27
3	25	25	0	600	23

AccuraSpray 4.0 for SPS

The single-point measurement system of the AccuraSpray 4.0, developed based on the validated prototype, was employed first to characterize first the in-flight particles under plasma conditions described in Test #3 in Table 1 for spray of 20 wt.% YSZ suspension. In a second series of experiments, the temperature and velocity of in-flight alumina particles sprayed with an axial injection plasma torch (Northwest Mettech Corp., Canada) a 3/8-in. nozzle diameter were characterized. An alumina powder (ZiBo.V.Gree. Trading, China) with an average particle size of 0.4 μm was put in suspension in ethanol with a concentration of the 20 wt.% powder with 1 wt.% polyvinylpyrrolidone (Sigma-Aldrich, USA) as a surfactant. The flow rate of alumina suspensions was kept constant at 45 mL/min for each set of experiments. Nitrogen with a flow rate of 15 mL/min was employed to atomize the suspension before entering the plasma. Table 2 shows spray conditions for these tests.

Temperature Sensitivity to Measurement Conditions

Effect of optical filtering, reflection from surrounding walls (or other objects in the spray booth), and direct plasma radiation was investigated. For this series of tests, YSZ suspension was sprayed with the 3 MB torch operated in Test #3 conditions (Table 1). Both the raw signals at the photodetector and measured temperature were compared for this spray condition. To understand the effect of optical filtering, the signal and temperature were recorded by using regular optical filters of the AccuraSpray 4.0 and compared to an enhanced filter configuration. The enhanced filter was composed of two customary filters with OD 6 which they were stuck together for more effective blockage of the rejected wavelengths. To investigate effect of the reflection from surrounding walls in the spray booth, a light beam dump was employed to reduce the intensity of the radiation that would reach the sensor. The beam dump was a mat black closed-end cylinder of 10 cm in diameter. The beam dump was placed in front of the diagnostic system to prevent reflection of radiation from the plasma or other sources on the surrounding booth walls from entering the

Table 2 Plasma conditions for spraying the alumina suspension with the Mettech torch

Test #	Gas flow rate, L/min			Current, A	Power, kW
	Ar	N_2	H_2		
4	184	23	23	180	90

diagnostic system. The raw signal and temperature were recorded in the presence and absence of the beam dump. Finally, to understand the effect of direct plasma radiation on the measurement, a shield was placed between the plasma and the diagnostic system to mask the plasma in the sensor field of view. The beam dump was built by a cylindrical tube and plate coated with a mat black paint to trap the reflected light. The size of the assembly was larger enough to cover the whole field of view of the sensor. We made a steel shield and positioned it at around 5 cm from the side of the torch. The shield had to be light enough so it could be mounted on the torch and be moved along with the robot arm. The width of the shield was 10 cm in order to shield the camera sensors from direct plasma light. The signal and temperature were recorded with and without the shield.

Results and Discussion

Characterizing YSZ in SPS by AccuraSpray G3C and the Prototype

AccuraSpray G3C and the prototype were used to measured temperature of in-flight particles in SPS. Figure 3 shows the temperature of in-flight YSZ particles as a function of plasma power at a standoff distance of 60 mm from the torch exit obtained with the double-point measurement system and single-point prototype. The double-point measurement system displayed significantly higher temperature readings, reaching 3460 °C at a plasma power of 34 kW, while the single-point measurement prototype measured 3140 °C for the same condition. The offset between the two readings at 34 kW was 320 °C, and it stayed as high as 260 °C for the lower plasma power set point (23 kW).

Figure 4 presents the temperature readings from the double-point measurement system and single-point

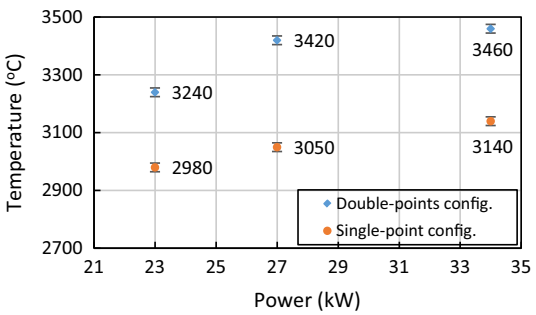

Fig. 3 Temperature of YSZ in-flight particles measured by the double-point measurement system and single-point measurement prototype in SPS process at 60 mm standoff distance of the 3 MB torch

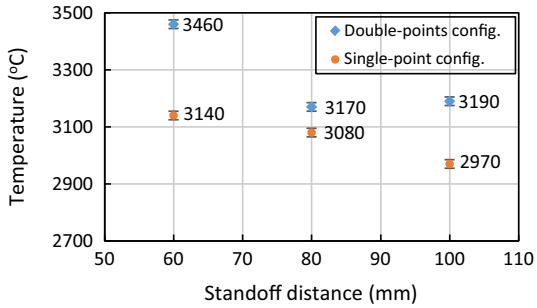

Fig. 4 Temperature of YSZ in-flight particles measured by the double-point measurement system and single-point measurement prototype in SPS process for the condition of high power (Test #1) with the 3 MB torch

measurement prototype at three different spray distances with the plasma power set to 34 kW. Temperature readings of the single-point measurement system show a continuously decreasing trend with the spray distance as expected. For the double-point measurement, the temperature decrease was observed up to 80 mm, and then, the temperature starts to increase at a longer standoff distance. Such a temperature increase is a measurement artifact as the temperature of the spray particles should decrease with the spray distance. Indeed, there is no exothermic reaction between the zirconia particles and the plasma or surrounding air as the material is already oxidized. The same figure shows that the two-point measurement system systematically measured temperatures that were higher than the single-point measurement configuration. This difference was around 320 °C at a standoff distance of 6 cm and around 90 °C at the 8 cm.

To the best of the authors' knowledge, the two-color pyrometry is the only practical method to measure the in-flight particle temperature in thermal spray processes. In this technique, the measurement volumes probed at the two selected wavelengths are normally totally superimposed (simple-point measurement). The double-point measurement approach is subject to additional measurement errors if, for example, the particle temperature and their number density as well as plasma radiation are different in the two distinct measurement volumes. Consequently, the single-point measurement approach is expected to be more reliable than the double-point approach. This is consistent with the results of Fig. 4 showing that the particle temperature decreases continuously with distance in the single-point configuration (Fig. 4) as expected. The exact reasons explaining the higher temperatures measured in the double-point configuration are not fully clear to the authors at this time.

As shown in Fig. 4, the slope of the particle temperature with distance as measured by the prototype is relatively low. This can be caused by a bias of measurements toward

the relatively larger and hotter particles. These particles have stronger radiation and slower cooling rates, and they have a noticeable influence on the average temperature recorded by the system.

Analyses of Collected YSZ Splats from SPS

Figure 5 shows the particle temperature as a function of standoff distance from the torch exit in the Test 3 condition. For this test, a low power condition was selected to avoid large overheating of the particles where they would cool down below their melting point along the spray axis. The goal was to collect splats at different standoff distances where particles temperature was expected to be above the melting point for the shorter spray distance and below the melting point for the farthest standoff. The measurement shows that the most noticeable temperature changes were between the standoff distances of 30 and 40 mm where the temperature dropped almost 200 °C. The rapid initial temperature drop can be associated more with the stray radiation than the natural temperature decrease in the particles. Fazilleau et al. (Ref 37) showed the temperature of plasma drops considerably (independent of gas type) at close axial distances. However, it remains as high as 4000 °C at standoff distance of around 5 cm. Therefore, the particles cannot experience a sharp temperature drop because of the plasma cooling. Delbos et al. (Ref 26) studied heat transfer for the particles. Assuming the radiative heat transfer between the plasma and particles was in balance as far as 4 cm, convection heat transfer was the dominant mechanism for cooling down of particles. The heat transfer through convection is proportional to temperature difference. For this analysis it was assumed, the convection coefficient was constant. This means than the temperature drop should be linked to the convection which changes linearly with temperature. On the other hand, the level of stray radiation from the plasma was higher close to the torch. Spectroscopic measurements (Ref 29) showed that the irradiance from free charges and ions in the plasma covers the whole spectrum in the visible and near-infrared (NIR) ranges. This irradiance was higher closer to the torch, and it diminished with the measurement distance from the torch. Therefore, it is concluded that the reading of a high temperature at 30 cm was due to the stray radiation which added to the thermal radiation from particles. At standoff distances larger than 40 cm, the rate of cooling was around 25 °C/cm. The cooling rate decreased as the measurement volume was farther from the torch and it increased for a higher power plasma. The results obtained using the single-point measurement prototype seemed promising; nevertheless, it required to be verified indirectly through the splats studies.

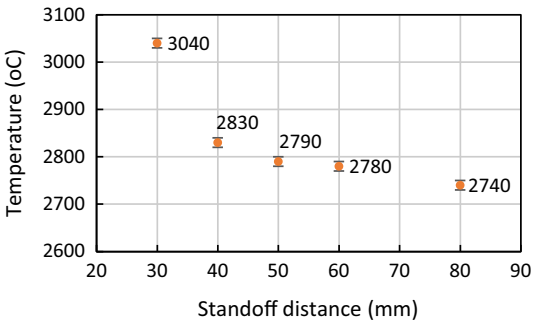

Fig. 5 Temperature of YSZ in-flight particles measured by prototype in SPS process for the condition of low power (Test #3) with 3 MB torch

Figure 6 depicts the SEM images of splat samples collected at different spray distances. At 30 mm, the glass substrate was totally covered with the splats which meant relatively high deposition efficiency. The number of splats was countless, and the shape of splats illustrated that most particles were entirely molten at the impact. At this point, the device recorded an average particles temperature of 3040 °C which was over the melting point of the YSZ. At 40 mm, the glass substrate was more visible which indicates that a smaller number of particles had enough energy to successfully impact and attach to the substrate. Furthermore at a standoff distance of 40 mm, fewer number of splats smaller than 1 μm were observed compared to the spray distance of 30 mm. The temperature measured by the sensor at 40 mm was 2830 °C which was very close to the YSZ melting point (2800 °C) (Ref 38). As the spray distance increased to 50 and 60 mm, the deposited area on the glass substrate reduced and the shape of splats tended toward thicker well-developed disks. Moreover, the number of spherical particles with diameter ranging between 0.5 and 1 μm was observed at 60 mm. These spheres were most likely partially resolidified in-flight particles which impinged on the substrate. However, the impact did not deform their shapes as they were partially solid. The minimum diameter of the splats at 50 mm was around 1 μm. At that distance, the diagnostic device measured temperatures around 2780 °C which is marginally below the melting point of the material. At 80 mm, most of the particles reached the substrate in the form of resolidified spheres except relatively large particles. At this distance, no flatten splats smaller than 1.5 μm can be observed and the number of collected splats was countable. Tendency of splats to conserve their spherical shape supported this idea that they were semi-molten. The temperature of in-flight particles was 2740 °C at 80 mm away from the torch.

As discussed above, the density of collected splats on the glass plates decreases rapidly with increased spray distance. The observation of the number of particles retained on the glass substrate at 5 cm shows a

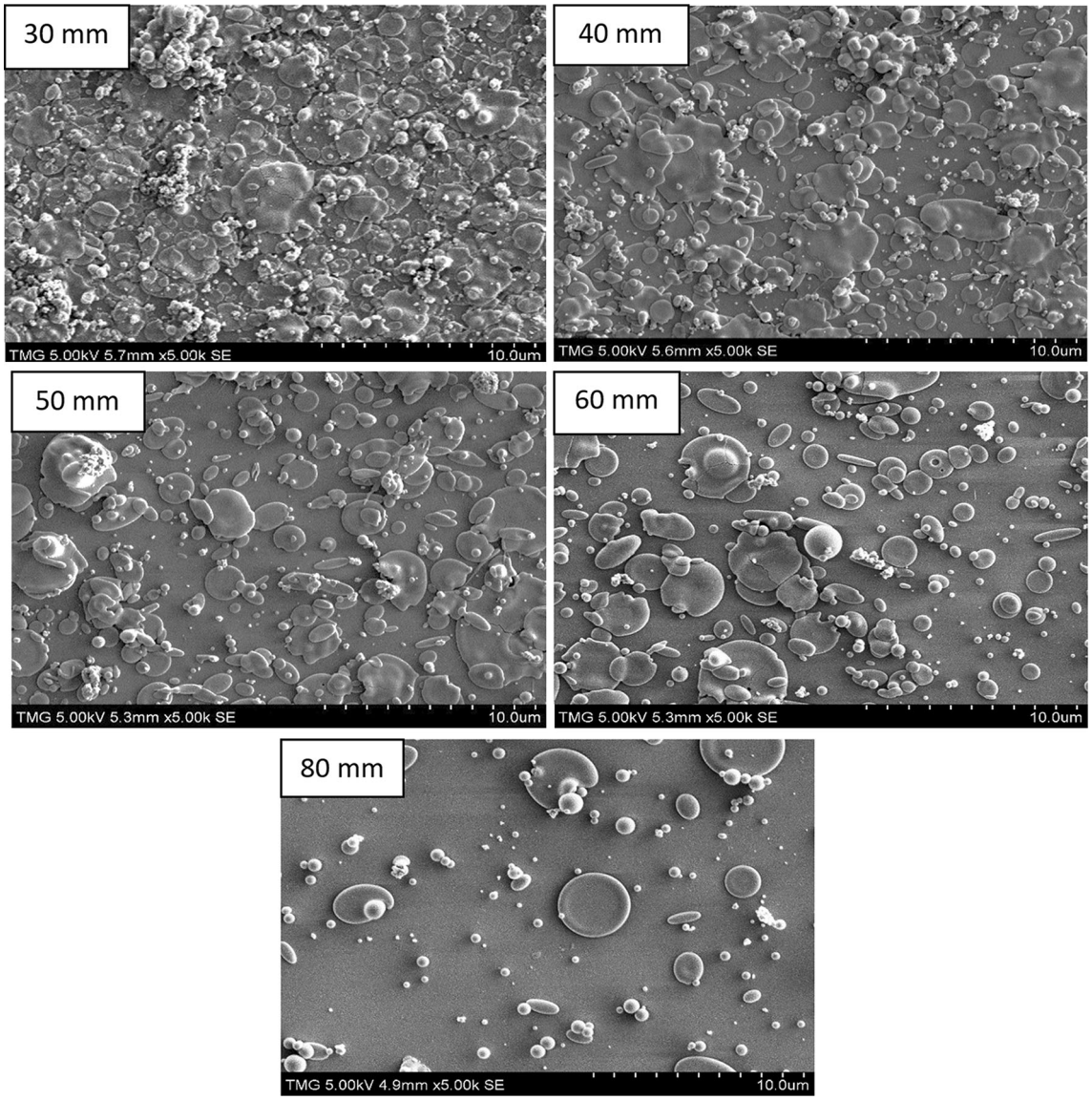

Fig. 6 SEM images of YSZ splats at the glass substrates for five spray distances from 30 to 80 mm for condition of low power (Test #3) in SPS process with 3 MB torch

considerable amount of small resolidified particles. It is believed that due to their small size and momentum, such particles could not be collected at a distance of 8 cm. It is a reasonable assumption to consider particles as a point source which are distributed uniformly. The number of particles per unit of the surface area counted on the glass substrate depends on the distance from the source. For a stationary torch and a fixed sampling glass substrate, the number of particles on the substrate is reduced proportional to the inverse of the squared distance. However, as the torch scanned the substrate in our case, the number of particles on the substrate should be reduced proportional to the inverse of the distance. The ratio of the particle number at 8 and 5 cm was calculated by counting the number of particles in the same area of interest at the two distances. It was found that the number of particles counted at 8 cm was much less than the number of particles calculated from the number particles at 5 cm times the ratio of distance. In short, this was an indication that fewer particles could reach and stick to the substrate because of rapid cooling down and velocity reduction. Moreover, the diagnostic device makes ensemble measurements which covers the full range of particle size and temperature distributions. In fact, it gave an average temperature value of all the particles that passes through its measurement volume with a bias toward hotter and larger particles as they emit higher intensity of thermal radiation. Observation of few small splats collected on the substrate confirmed that the smaller

particles of the distribution were at lower temperature than the melting point. Upon an impact on the substrate, these smaller particles were resolidified and they consequently bounced back. At spray distance of 80 mm, the double-point measurement system showed a temperature around 2890 °C which was considerably higher than the melting point of the material. The physical reason that the double-point measurement overestimates the temperature is $I_{\lambda 2\ \text{measurement}}$ was less than $I_{\lambda 2\ \text{real}}$ and this resulted that $(I_{\lambda 1}/I_{\lambda 2})_{\text{measurement}}$ was larger than $(I_{\lambda 1}/I_{\lambda 2})_{\text{real}}$. Consequently, the temperature calculated from Eq. 3 by a larger emission ratio at two wavelengths overestimated the real temperature. Therefore, the result of the double-point measurement system was in contradiction to the information achieved from studying of splats through the SEM. To summarize, evolution of temperature along the spray axis was consistent with the evidence achieved from analysis of the micrographs. The splat analysis confirmed credibility of temperature reading by the single-point measurement prototype.

Sensitivity Analysis of Temperature to Measurement Conditions

The objective of this section is to report on the sensitivity of temperature measurements on the spray environment and improved filtering used in the AccuraSpray 4.0. In fact, this diagnostic system is the independent product further developed based on the prototype investigated this study to measure both the temperature and velocity of particles. Figure 7 shows the raw signals from the temperature detector of $_1$ in six different measurement conditions collected with the same spray conditions (Test 3). Depending on the measurement condition, the voltage amplitude of the detected signal was different. In other words, the surrounding booth and stray radiation could have an impact on the detected signals. A more detailed analysis was carried out by looking at the root-mean-square (RMS) value of the signals to better understand the effects of measurement conditions.

Figure 8 shows the RMS signal value for each case. The reference condition was Case 4 without the shield, no the light dump, and the normal filtering. Table 3 reveals percentage of changes in the RMS values when each of three mentioned options was added to the test setup. The enhanced filter reduced the RMS value between 20 and 30% compared to the standard filters used in the diagnostic system. The reduction in the RMS could be as a result of an unfavorable signal attenuation of the in-flight particles in the transmission band of the filter and as a result of more effective blockage of the stray radiation out of the transmission band. Between these two, higher blockage of unwanted wavelengths of the spectrum by the filter reduced the RMS value more significantly. In the other case, employing the light beam dump reduced the RMS value between 4 and 5% which means that the reflections from the booth had a small effect the signal. Finally, using the shield between the plasma and the diagnostic system reduced the RMS by 1%. Analysis of RMS value provided an indicator to assess the effects of measurement

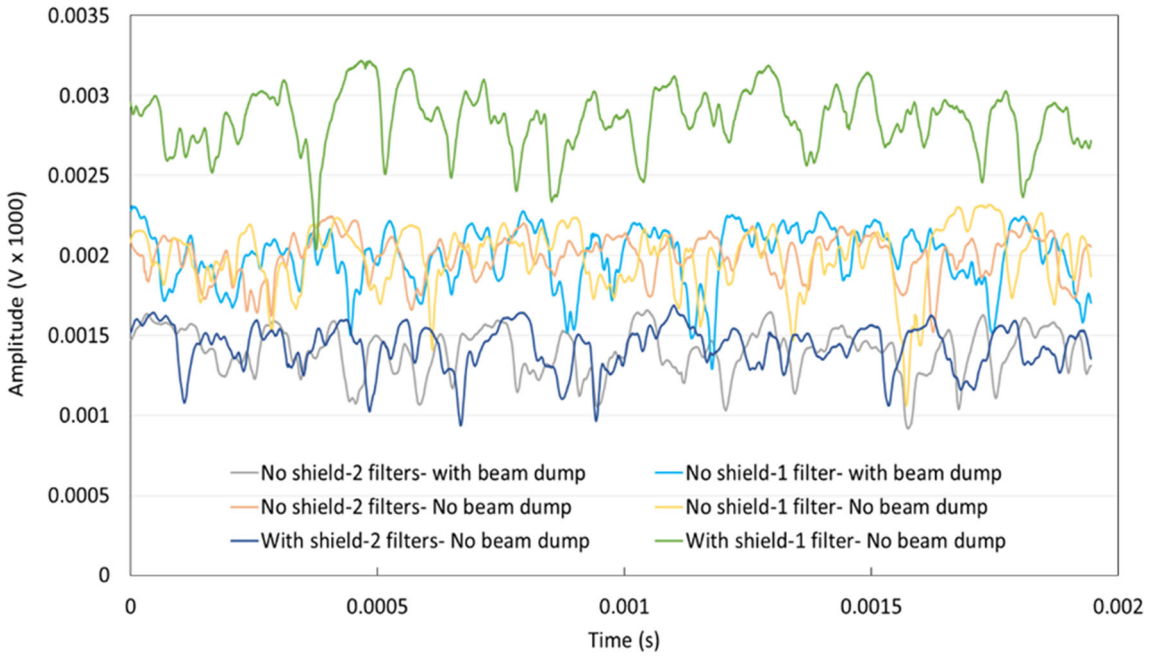

Fig. 7 Voltage amplitude at the temperature detector for the six measurement conditions at spray condition test #3

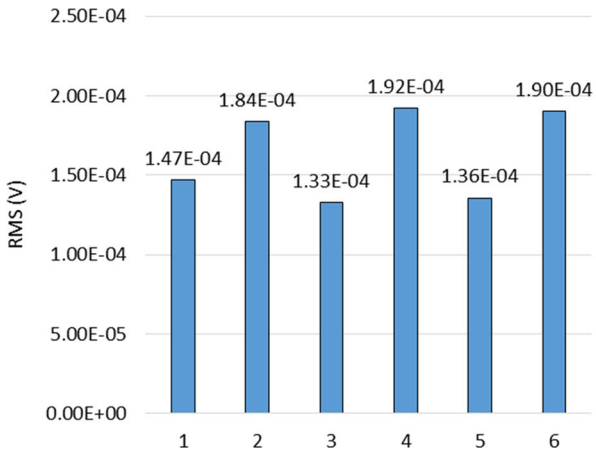

	Measurement condition		
Condition No.	Plasma shield	Enhanced filter	Beam dump
1	No	Yes	Yes
2	No	No	Yes
3	No	Yes	No
4 (reference)	No	No	No
5	Yes	Yes	No
6	Yes	No	No

Fig. 8 RMS of signal amplitude for six measurement conditions at the spray condition #3

Table 3 Reduction in RMS value for each of three added elements to the test setup

Effect	RMS reduction, %
Enhanced filter	20-30
Beam dump	4-5
Plasma shield	1-2

conditions on the measured temperature. This analysis is more tangible when measured temperature was considered for each measurement condition.

Figure 9 shows the temperature reading for each of the measurement conditions as a function of the standoff distance. The trend of temperature changes as a function of standoff distances was the same for all test conditions. To elaborate more, the temperature at standoff distance of 50 mm is discussed in more detail below. The temperature at the reference condition (No. 4) was 2860 °C which was the highest of all measurement conditions. Temperature reading obtained using the using the enhanced filters was 2820 °C. The measured temperature by the enhanced filter was 40 °C less which corresponds to the 20% lower RMS value. Regarding reflection effect, the temperature was 2840 °C (20 °C less than the reference condition) when the beam dump was employed. In the previous analysis, it was understood that the beam dump reduced the RMS value by 4%. If the plasma direct radiation was concerned, the temperature was 2830 °C when the shield protected the diagnostic system from the direct plasma radiation. In this case, a lower temperature of 20 °C was corresponded to 1% lower RMS value of the signal. Effect of the enhanced filter was more significant when the standoff distance was shorter as expected. At 30 mm from the torch, temperature of the reference condition was 2990 °C, whereas the temperature was 2870 °C for the case of using the enhanced filter. As shown in Fig. 10 for the same measurement, the velocity decreased from 470 m/s at 30 mm from the torch to around 240 m/s at 60 mm. This trend of changes was as expected and within a common range of velocity for typical plasma conditions in SPS. The result showed the velocity dropped at the rate of 70 m/s per 10 mm for standoff distance from 30 to 60 mm. As expected, one observes slower particles in a farther standoff distance because of the air drag. It is helpful to mention, although the temperature varied around 130 °C at 30 mm of the torch, the velocity had insignificant variation as the measurement condition changed as shown in Fig. 10. Similarly, the variation of velocity for different measurement conditions at the further standoff distances was insignificant. To summarize, the measurement condition changes the recorded temperature to a certain extent. Undesirable radiation of spectrum has a major effect on temperature measurements; however, its effect can be eliminated by using optical filters with the more effective blockage.

Characterizing Alumina in SPS by AccuraSpray 4.0

Performance of the single-point measurement system was investigated for a higher power plasma which produces more intense plasma radiation and consequently is more challenging for characterization of in-flight particles. For this purpose, temperature of alumina powder, injected to the plasma from the Mettech torch, was measured in the SPS process by the single-point measurement system. The Mettech torch can be operated at very high power. Figure 11 shows that the particles temperature decreased from 2700 to 2670 °C by sampling at two different standoff distances (50 and 75 mm). It means the particles experienced a drop of temperature around 30 °C by moving 25 mm.

It was predictable that temperature of particles would be lower at the farther distance; however, this drop was relatively small. This result can be explained by considering the melting point of alumina and plasma power at the

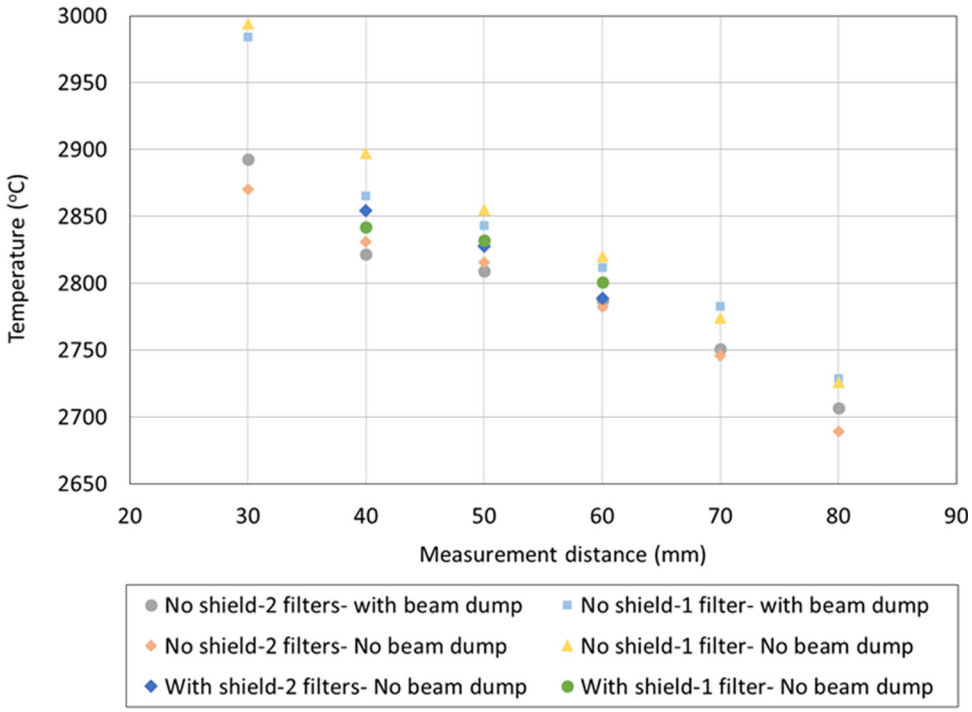

Fig. 9 Temperature of in-flight particles as a function of standoff distance six measurement conditions for the spray condition test #3, size of markers shows the standard deviation of measurement

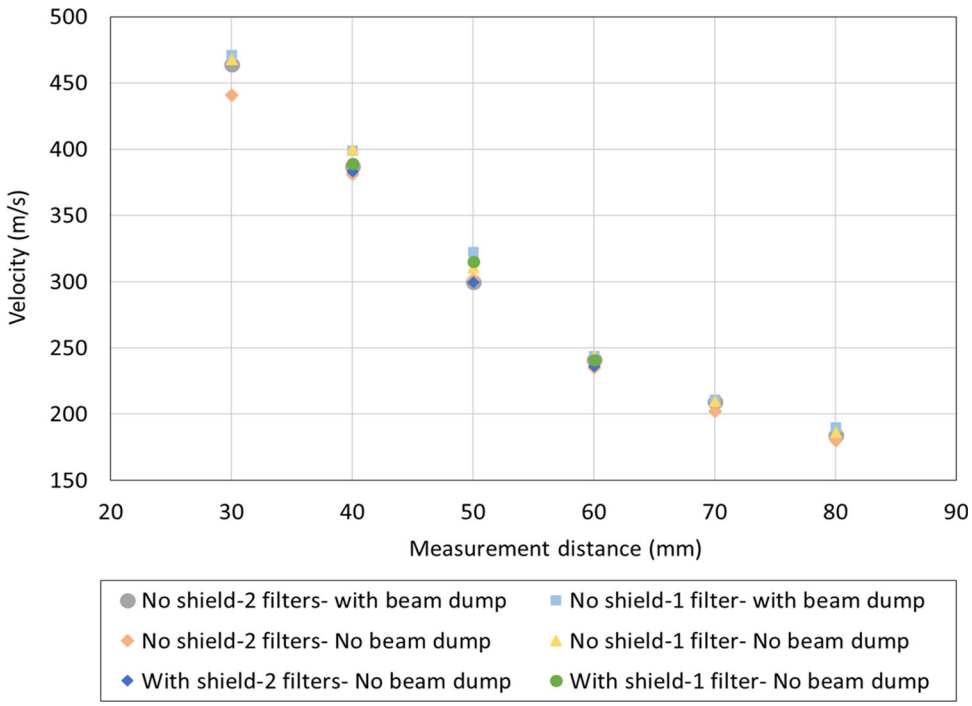

Fig. 10 Velocity of in-flight particles as a function of standoff distance six measurement conditions for the spray condition test #3, standard deviation of velocity is 3 m/s

measurement points. In fact, the melting point of alumina is around 2070 °C which is considerably lower than the plasma temperature in this experiment. Therefore, most of the axially injected particles got fully molten in the heat of plasma. On the other hand, the length of the plasma plume from the exit of the torch was over 75 mm. It was an indicator that both measurements were conducted in the hot zone which had a small temperature gradient along the plume. This was in an agreement with the measurement. Velocity of in-flight particles drops from 669 to 643 m/s which was expected for the spray condition. Tarasi et al. (Ref 28) reported a temperature around 2900 °C and a velocity around 610 m/s for a similar spray condition of alumina and YSZ mixture measured by the double-point

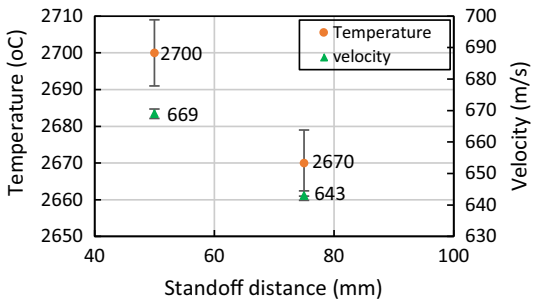

Fig. 11 Temperature and velocity of alumina in-flight particles measured by the single-point measurement system in SPS process for the condition of Test #4 with the Mettech torch

measurement system, AccuraSpray G3C. The temperature measured by the single-point measurement system was more realistic than the one measured by the double-point measurement system.

Statistical error was evaluated for measurement over a period of 50 s. The sampling rate for temperature measurement was 20 Hz. Standard deviation of temperature for this period and sampling was ± 1 °C. However, the main source of deviation in the measurement was due to the local positioning of the sensor (position of measurement volume relative to the spray). The uncertainty due to positioning causes an error estimated at ± 10 °C. This error is shown by error bars or size of markers in the figures.

Conclusions

The main objective of this work for development of a reliable system to measure temperature of in-flight particles in SPS and evaluation of the system was successfully achieved. Diagnostic system for the APS process known as AccuraSpray G3C, based on the double-point measurement system, can provide an estimation of in-flight particle temperature in SPS for spray distance between 50 and 80 mm, and it shows some deviation from expected temperature at shorter and longer spray distances. The deviation exists regardless of the plasma power. Furthermore, the double-point measurement configuration systematically overestimates the temperature of in-flight particles in SPS. Therefore, a new sensor configuration was further developed and adjusted exclusively for SPS to improve the accuracy of temperature measurement. A single-point measurement configuration and an improvement of the signal filtering were applied in the new system. The result of temperature measurements in SPS was indirectly verified through the splat analysis. The splat analysis was consistent with the evolution of temperature measured by the single-point measurement prototype. The SEM images of splats showed that most of the particles were resolidified and they did not flatten nor stuck to the substrate when the sensor measured temperature of particles to be below the melting point. Moreover, effect of measurement conditions on temperature of particles was investigated. The study showed the stray radiation has limited influence on the temperature measurement in the condition of this work. Elimination of stray radiation with using components such as an enhanced filter, a beam dump, and a shield provides more realistic temperature of in-flight particles particularly at a shorter spray standoff distance. Applying these components can be necessary to avoid significant bias on the temperature measurements for some spray and measurement conditions. In short, due to reduction in the measurement volume and optimized filtering, AccuraSpray 4.0 based on the single-point measurement configuration can successfully measure the temperature of the in-flight particles in SPS.

Acknowledgments The authors gratefully acknowledge Morvarid Mohammadian and Saeid Garmeh for their kind help to carry out the experiments and for their fruitful discussion on the topic. This project was funded by the Natural Sciences and Engineering Research Council of Canada (NSERC), Canada Research Chair, and Mitacs program.

References

1. H. Kassner, R. Siegert, D. Hathiramani, R. Vassen, and D. Stoever, Application of Suspension Plasma Spraying (SPS) for Manufacture of Ceramic Coatings, *J. Therm. Spray Technol.*, 2008, **17**, p 115-123
2. G. Mauer, A. Guignard, R. Vaßen, and D. Stöver, Process Diagnostics in Suspension Plasma Spraying, *Surf. Coat. Technol.*, 2010, **205**, p 961-966
3. C. Moreau, J. Bisson, R. Lima, and B. Marple, Diagnostics for Advanced Materials Processing by Plasma Spraying, *Pure Appl. Chem.*, 2005, **77**, p 443-462
4. S. Sampath, V. Srinivasan, A. Valarezo, A. Vaidya, and T. Streibl, Sensing, Control, and In Situ Measurement of Coating Properties: An Integrated Approach Toward Establishing Process-Property Correlations, *J. Therm. Spray Technol.*, 2009, **18**, p 243-255
5. O.P. Solonenko, Complex Investigation of Thermophysical Processes in Plasma-Jet Spraying, *Pure Appl. Chem.*, 1990, **62**, p 1783-1800
6. S. Coulombe and M. Boulos, In-Flight Particle Diagnostics in Induction Plasma Processing, *Plasma Chem. Plasma Process.*, 1995, **15**, p 653-675
7. M. Vardelle, A. Vardelle, P. Fauchais, and M. Boulos, Plasma—Particle Momentum and Heat Transfer: Modelling and MEASUREMENTS, *AIChE J.*, 1983, **29**, p 236-243
8. J. Fincke, C. Jeffery, and S. Englert, In-Flight Measurement of Particle Size and Temperature, *J. Phys. E Sci. Instrum.*, 1988, **21**, p 367
9. J.R. Fincke, W.D. Swank, R.L. Bewley, D.C. Haggard, M. Gevelber, and D. Wroblewski, Diagnostics and Control in the Thermal Spray Process, *Surf. Coat. Technol.*, 2001, **146**, p 537-543
10. J. Mishin, M. Vardelle, J. Lesinski, and P. Fauchais, Two-Colour Pyrometer for the Statistical Measurement of the Surface

Temperature of Particles Under Thermal Plasma Conditions, *J. Phys. E Sci. Instrum.*, 1987, **20**, p 620
11. P. Fauchais, G. Montavon, M. Vardelle, and J. Cedelle, Developments in Direct Current Plasma Spraying, *Surf. Coat. Technol.*, 2006, **201**, p 1908-1921
12. G. Mauer, R. Vaßen, and D. Stöver, Plasma and Particle Temperature Measurements in Thermal Spray: Approaches and Applications, *J. Therm. Spray Technol.*, 2011, **20**, p 391-406
13. G. Mauer, R. Vaßen, S. Zimmermann, T. Biermordt, M. Heinrich, J. Marques, K. Landes, and J. Schein, Investigation and Comparison of In-Flight Particle Velocity During the Plasma-Spray Process as Measured by Laser Doppler Anemometry and DPV-2000, *J. Therm. Spray Technol.*, 2013, **22**, p 892-900
14. J. Blain, F. Nadeau, L. Pouliot, C. Moreau, P. Gougeon, and L. Leblanc, Integrated Infrared Sensor System for On Line Monitoring of Thermally Sprayed Particles, *Surf. Eng.*, 1997, **13**, p 420-424
15. P. Gougeon, C. Moreau, V. Lacasse, M. Lamontagne, I. Powell, and A. Bewsher. A New Sensor for on-line Diagnostics of Particles Under Thermal Spraying Conditions. Advanced Processing Techniques, C. Lall and A.J. Neupaver (Eds), *International Conference on Powder Metallurgy and Particulate Materials*, Toronto, Canada, Metal Powder Industries Federation, APMI, 1994, p 199-210
16. C. Moreau, P. Gougeon, M. Lamontagne, V. Lacasse, G. Vaudreuil, and P. Cielo. On-Line Control of the Plasma Spraying Process by Monitoring the Temperature, Velocity, and Trajectory of In-Flight Particles, in *Thermal Spray Industrial Applications*, C.C. Berndt and S. Sampath (Eds.), *Proceedings National Thermal Spray Conference*, 20-24 June 1994, Boston, Mass., ASM International, 1994, p 431-437
17. C. Moreau, P. Gougeon, A. Burgess, and D. Ross. Characterization of Particle Flows in an Axial Injection Plasma Torch, Advances in Thermal Spray Science and Technology, C.C. Berndt and S. Sampath (Eds.), *Proceedings National Thermal Spray Conference, Houston*, Texas, ASM International, 1995, p 141-147
18. J.F. Bisson, M. Lamontagne, C. Moreau, L. Pouliot, J. Blain, and F. Nadeau. Ensemble In-Flight Particle Diagnostics Under Thermal Spray Conditions, Thermal Spray 2001 New Surfaces for a New Millennium, *Proceedings of the International Thermal Spray Conferences*, Singapore, ASM International, 28-30 May 2001, p 705-714
19. A. Killinger, R. Gadow, G. Mauer, A. Guignard, R. Vaßen, and D. Stöver, Review of New Developments in Suspension and Solution Precursor Thermal Spray Processes, *J. Therm. Spray Technol.*, 2011, **20**, p 677
20. G. Mauer, R. Vaßen, and D. Stöver, Comparison and Applications of DPV-2000 and Accuraspray-g3 Diagnostic Systems, *J. Therm. Spray Technol.*, 2007, **16**, p 414-424
21. J. Vattulainen, E. Hämäläinen, R. Hernberg, P. Vuoristo, and T. Mäntylä, Novel Method for In-Flight Particle Temperature and Velocity Measurements in Plasma Spraying Using a Single CCD Camera, *J. Therm. Spray Technol.*, 2001, **10**, p 94-104
22. J.E. Craig, R.A. Parker, D.Y. Lee, F. Biancaniello, and S. Ridder, A Two-Wavelength Imaging Pyrometer for Measuring Particle Temperature, Velocity and Size in Thermal Spray Processes, *Proceedings of the International Symposium on Advanced Sensors for Metals Processing, Annual Conference of Metallurgists of CIM, Gateway to the 21st Century*, Quebec City, PQ, Canada, 22-26 August 1999, p 369-380
23. S.P. Mates, D. Basak, F.S. Biancaniello, S.D. Ridder, and J. Geist, Calibration of a Two-Color Imaging Pyrometer and Its Use for Particle Measurements in Controlled Air Plasma Spray Experiments, *J. Therm. Spray Technol.*, 2002, **11**, p 195-205
24. D. Wroblewski, G. Reimann, M. Tuttle, D. Radgowski, M. Cannamela, S. Basu, and M. Gevelber, Sensor Issues and Requirements for Developing Real-Time Control for Plasma Spray Deposition, *J. Therm. Spray Technol.*, 2010, **19**, p 723-735
25. A. McDonald, C. Moreau, and S. Chandra, Use of Thermal Emission Signals to Characterize the Impact of Fully and Partially Molten Plasma-Sprayed Zirconia Particles on Glass Surfaces, *Surf. Coat. Technol.*, 2010, **204**, p 2323-2330
26. C. Delbos, J. Fazilleau, V. Rat, J. Coudert, P. Fauchais, and B. Pateyron, Phenomena Involved in Suspension Plasma Spraying Part 2: Zirconia Particle Treatment and Coating Formation, *Plasma Chem. Plasma Process.*, 2006, **26**, p 393-414
27. Z. Zeng, S. Kuroda, and H. Era, Comparison of Oxidation Behavior of Ni-20Cr Alloy and Ni-Base Self-Fluxing Alloy During Air Plasma Spraying, *Surf. Coat. Technol.*, 2009, **204**, p 69-77
28. F. Tarasi, M. Medraj, A. Dolatabadi, J.O. Berghaus, and C. Moreau, Amorphous and Crystalline Phase Formation During Suspension Plasma Spraying of the Alumina-Zirconia Composite, *J. Eur. Ceram. Soc.*, 2011, **31**, p 2903-2913
29. B. Aziz, P. Gougeon, and C. Moreau, Temperature Measurement Challenges and Limitations for In-Flight Particles in Suspension Plasma Spraying, *J. Therm. Spray Technol.*, 2017, **26**, p 695-707
30. R. Vaßen, H. Kaßner, G. Mauer, and D. Stöver, Suspension Plasma Spraying: Process Characteristics and Applications, *J. Therm. Spray Technol.*, 2010, **19**, p 219-225
31. A. Cengel, HEHT TRANSFER, 2007.
32. F.W. Sears, M.W. Zemansky, and H.D. Young, *University Physics*, Addison-Wesley, Reading, 1987
33. G. Mauer, R. Vaßen, and D. Stöver, Detection of Melting Temperatures and Sources of Errors Using Two-Color Pyrometry During In-Flight Measurements of Atmospheric Plasma-Sprayed Particles, *Int. J. Thermophys.*, 2008, **29**, p 764-786
34. Y.S. Touloukian, and D.P. DeWitt, *Thermophysical Properties of Matter, The TPRC Data Series, Volume 8, Thermal radiative properties Nonmetallic Solids*, TEPIAC Publication, 1972, p 526-544
35. J. Manara, R. Brandt, J. Kuhn, J. Fricke, T. Krell, U. Schulz, M. Peters, and W.A. Kaysser, Emittance of Y_2O_3 Stabilised ZrO_2 Thermal Barrier Coatings Prepared by Electron-Beam Physical-Vapour Deposition, *High Temperatures High Pressures*, 2000, **32**, p 361-368
36. P. Coates and D. Lowe, *The Fundamentals of Radiation Thermometers*, CRC Press, Boca Raton, 2016
37. J. Fazilleau, C. Delbos, V. Rat, J. Coudert, P. Fauchais, and B. Pateyron, Phenomena Involved in Suspension Plasma Spraying Part 1: Suspension Injection and Behavior, *Plasma Chem. Plasma Process.*, 2006, **26**, p 371-391
38. https://www.Oerlikon.Com/ecomaXL/Files/Metco/oerlikon_DSMTS-0001.10_8YO_ZrO_HOSP.Pdf&download=1.